Measurement of mechanical resonance and losses in nanometer scale silicon wires

Dustin W. Carr,[a] S. Evoy, L. Sekaric, H. G. Craighead, and J. M. Parpia
Cornell Nanofabrication Facility and the Cornell Center for Materials Research, Cornell University, Ithaca, New York 14853

(Received 15 April 1999; accepted for publication 17 June 1999)

We present data on nanofabricated suspended silicon wires driven at resonance. The wires are electrostatically driven and detected optically. We have observed wires with widths as small as 45 nm and resonant frequencies as high as 380 MHz. We see a strong dependence of the resonant quality factor on the surface to volume ratio. © *1999 American Institute of Physics.* [S0003-6951(99)00633-6]

Mechanically resonant structures are of interest for a wide range of sensing applications[1–3] as well as basics physics research.[4] Deflecting cantilevers and beams have been thoroughly studied for their uses as resonant sensors.[5] The fabrication of smaller structures with lower mass and higher frequency can improve the sensitivity of such sensors. In this study, we have fabricated and measured the smallest (~50 nm wide) and highest frequency (380 MHz) resonant silicon structures reported in the literature.

Inelastic loss mechanisms have also been studied for structures over various length scales from millimeter size to several microns in size. As these structures become smaller the quality factor (Q factor) of the resonance decreases.[6–9] We show experimental results that display a strong dependence of the Q factor on the surface to volume ratio of the suspended silicon structures over a size region that has previously been unexplored.

A thorough description of the techniques of fabrication and measurements has been given before.[10,11] Previously we have studied larger, more complex suspended structures.

We use silicon on insulator (SOI) wafers to make all of the structures. All of these wafers have a buried oxide thickness of 400 nm and a silicon thickness of 200 nm. The structures are fabricated using electron beam lithography to define a pattern in a polymethyl(methacrylate) resist on the SOI wafers. We then perform an evaporation and liftoff of a Cr etch mask, followed by a reactive ion etch in a CF_4–H_2 plasma to etch through the top silicon layer. A wet etch in hydrofluoric acid is then used to undercut and release the wires. Thin layers of Cr (5 nm) and Au (10 nm) are then evaporated onto the surface, and contact is made by bonding aluminum wires to the top and bottom silicon layers.

The structure is mounted in a small vacuum chamber which is maintained below 1 mTorr. The chamber is mounted on a three axis stage that uses manually adjusted micrometers for precise positioning. A helium neon laser is focussed onto the structure using a microscope objective. All measurements are performed at room temperature. The reflected signal is detected using a silicon photodetector. The output from the photodector is passed through an integrated ac-coupled preamplifier. The signal output from the preamp is measured with the spectrum analyzer. The devices are driven using the rf output from the spectrum analyzer that is added to a dc offset voltage. The dc voltage is necessary in order to have a response that is at the same frequency as the driving signal because the force on the structures depends on the square of the voltage.

As the wires move, the intensity of scattered light that is incident on the photodetector changes. The interaction of the light with the structure is not easily understood. We have explored the interaction with boundary element analysis in order to understand the modulation of the scattered light, as well as effects due to optical pressure and heating from the laser.[12] From experiment, we have seen that the measured signal is linear with the applied voltage, indicating that the signal we measure is linear with the oscillation amplitudes for small amplitudes.

A typical test structure is shown in Fig. 1. This is a harp-like array of single wires. The wires vary in length between 8 and 1 μm with steps of 1 μm. The whole structure is repeated several times with different wire widths. The wires are sufficiently separated in length as to eliminate any overlapping of the fundamental modes. While we did detect higher order modes, we did not study any modes other than the fundamental.

We detected the resonance of wires with lengths between 8 and 2 μm. Wires with lengths below 2 μm could not be easily detected. The frequency of suspended wires that are not under tension should vary according to the relation

$$\omega=\left(\frac{4.73}{l}\right)^2\left(\frac{EI}{\rho A}\right)^{1/2}, \tag{1}$$

where A is the cross-sectional area, I is the second moment of inertia, l is the length, E is the Young's modulus of the material, and ρ is the density of the material. The wires do behave as expected up to a frequency of 380 MHz.

Previous researchers have used Lorentz forces to drive and detect small oscillators.[13] The optical measurement technique discussed here demonstrates a signal to noise that is at least as good as that achieved with the Lorentz force measurements. Figure 2 shows a typical curve of the response of one of the wires with a resonant frequency of 225 MHz. This wire was 2 μm long$\times$100 nm$\times$100 nm. Even at this fre-

[a]Electronic mail: dwc5@cornell.edu

 © 1999 American Institute of Physics
Downloaded 17 Feb 2002 to 132.236.61.16. Redistribution subject to AIP license or copyright, see http://ojps.aip.org/aplo/aplcr.jsp

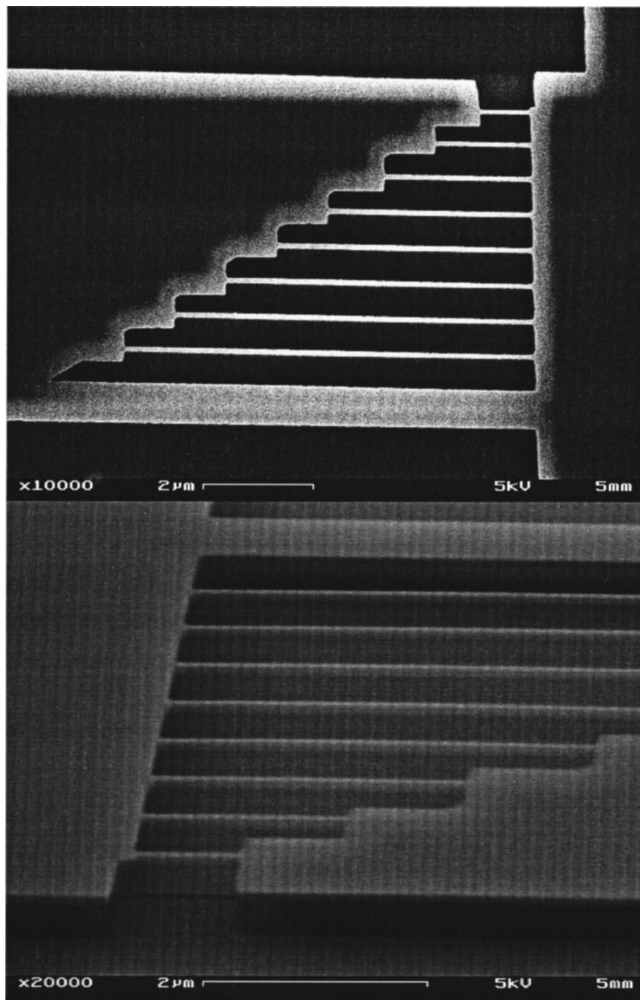

FIG. 1. Harp structure used in the measurements. The lengths of the wires vary between 1 and 8 μm. The center-to-center spacing of the wires is 630 nm.

quency, the signal to noise ratio is very high. We have detected a resonance in a 2 μm$\times$200 nm thick$\times$100 nm wire that was at 380 MHz.

Studying the Q factor as a function of the wire width

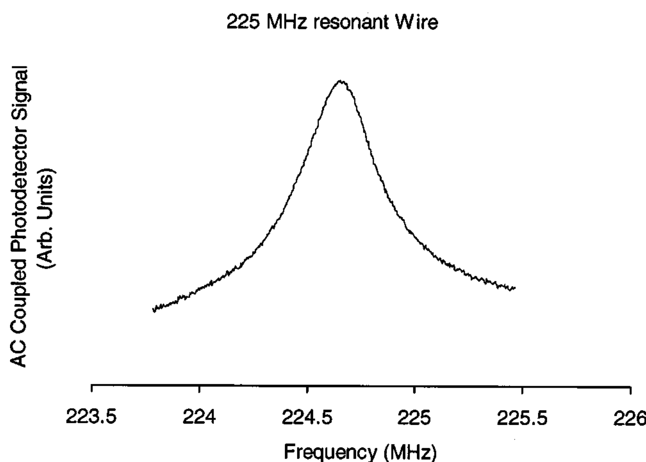

FIG. 2. Response curve of a 2 μm long wire with a 225 MHz fundamental mode frequency. The curve is acquired by sweeping the driving signal across a range of frequencies, and detecting the optical modulation at the same frequency using an ac coupled photodetector in combination with a spectrum analyzer.

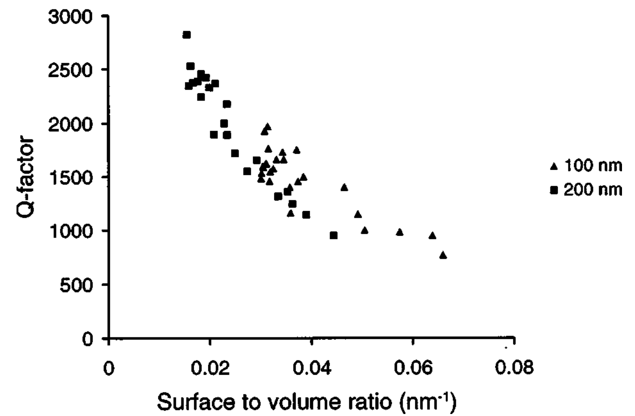

FIG. 3. Plot of the Q factor as a function of the surface to volume ratio. Two different wire thicknesses are shown, with several different wire widths for each thickness.

may help us to understand the loss mechanisms of structures on this size scale. As the surface to volume ratio increases, losses due to surface-related effects should increase, i.e., the Q factor should decrease as the wire dimensions decrease. Figure 3 shows a plot of the Q factor versus the surface to volume ratio, showing just such a behavior. The points on the plot are from wires of two different thicknesses. For the 200 nm thick structures, the wire width varies between 50 and 350 nm. For the 100 nm thick structures the wire width varies between 45 and 200 nm.

The exact nature of these losses is difficult to surmise. Certainly, the thin conductive films on the top surface of the wires do contribute somewhat to these losses. However, this film is very thin ($\sim$100 Å) compared to the silicon. Other authors have measured films with much thicker layers of Au on the surface, yet their measured Q factors are still greater than or equal to those measured here.[13,14] The Q factor dependence shown in Fig. 3 remains fairly continuous for two different thicknesses of the silicon. This tends to support the idea that all of the losses are related to the surfaces. Such surface losses could certainly be related to the near-surface damage induced during the plasma etch. Further studies are necessary to understand the source of these losses.

We would like to comment on the sensitivity of this measurement technique. It is difficult to directly determine the exact amplitude of vibration of the resonant wires. We can get an estimate of this amplitude by looking at nonlinear effects. At large amplitudes, the restoring force becomes nonlinear due to stretching of the wire. This essentially adds a term in the force equation that is cubic in the deflection of the beam. This effect, along with potential applications has been thoroughly explored previously.[15,16] Such a term leads to a bistability in the beam, resulting in resonance curves like the ones shown in Fig. 4. As the frequency is swept from low to high, it reaches a point that is no longer stable and so it rapidly switches to the next stable state at a lower amplitude. The minimum amplitude at which this occurs is called the critical amplitude. This critical amplitude depends only upon the geometry of the vibrating beam. This relation is[5]

$$x_c = \frac{2h}{[0.5Q(1-\nu^2)]^{1/2}}, \quad (2)$$

Downloaded 17 Feb 2002 to 132.236.61.16. Redistribution subject to AIP license or copyright, see http://ojps.aip.org/aplo/aplcr.jsp

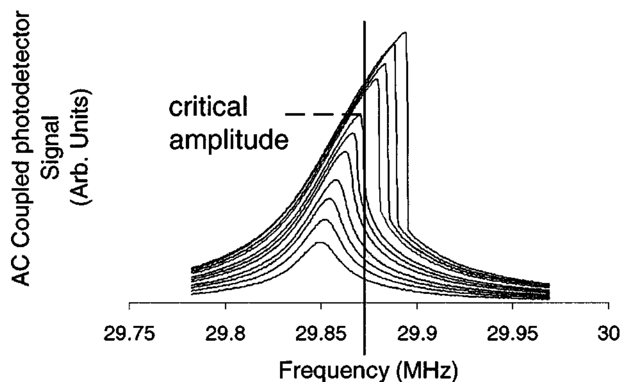

FIG. 4. Plot of the frequency response for various driving voltages. The point at which the response curve becomes bistable is indicated.

where h is the thickness of the wire in the direction of motion, and ν is the Poisson's ratio of the material. For the parameters of a typical wire, this amplitude is at most 20 nm. We can easily observe amplitudes that are 1/100 of this, indicating that we can detect a resonant well below 1 nm.

We have presented a technique for exciting and measuring mechanical resonance in silicon nanowires. The Q factor of these wires drops significantly as surface to volume ratio increases. The losses resulting in these low Q factors are probably surface related. In order to better understand the nature of these effects, we should carry out these experiments at a wide range of temperatures. All of the experiments to date have been performed at room temperature.

The measurement technique described is highly sensitive and is a useful tool for inspecting the behavior of these nanostructures. There are many more interesting experiments to attempt to help us to understand not only the mechanical behavior of these devices, but also their interaction with light.

[1] J. D. Zook, D. W. Burns, G. Guckel, J. J. Sniegowski, R. L. Engelstad, and Z. Feng, Sens. Actuators A **35**, 51 (1992).
[2] A. Prak, F. R. Blom, M. Elwenspoek, and T. S. J. Lammerink, Sens. Actuators A **25–27**, 691 (1991).
[3] C. Gui, R. Legtenberg, M. Elwenspoek, and J. H. Fluitman, J. Micromech. Microeng. **5**, 183 (1995).
[4] A. N. Cleland and M. L. Roukes, Nature (London) **392**, 160 (1998).
[5] H. A. C. Tilmans, M. Elwenspoek, and J. H. J. Fluitman, Sens. Actuators A **30**, 35 (1992).
[6] R. N. Kleiman, G. K. Kaminsky, J. D. Reppy, R. Pindak, and D. J. Bishop, Rev. Sci. Instrum. **56**, 2088 (1985).
[7] R. E. Mihailovich and J. M. Parpia, Phys. Rev. Lett. **68**, 3052 (1992).
[8] R. E. Mihailovich and N. C. MacDonald, Sens. Actuators A **50**, 199 (1995).
[9] D. W. Greywall, B. Yurke, P. A. Busch, and S. C. Arney, Europhys. Lett. **34**, 37 (1996).
[10] D. W. Carr and H. G. Craighead, J. Vac. Sci. Technol. B **16**, 3821 (1998).
[11] D. W. Carr and H. G. Craighead, J. Vac. Sci. Technol. B **15**, 2760 (1997).
[12] D. W. Carr and H. G. Craighead (unpublished).
[13] A. N. Cleland and M. L. Roukes, Appl. Phys. Lett. **69**, 2653 (1996).
[14] A. N. Cleland and M. L. Roukes, Sens. Actuators A **72**, 256 (1999).
[15] B. Yurke, D. S. Greywall, A. N. Pargellis, and P. A. Busch, Phys. Rev. A **51**, 4211 (1995).
[16] D. S. Greywall, B. Yurke, P. A. Busch, A. N. Pargellis, and R. L. Willet, Phys. Rev. Lett. **72**, 2992 (1994).

Downloaded 17 Feb 2002 to 132.236.61.16. Redistribution subject to AIP license or copyright, see http://ojps.aip.org/aplo/aplcr.jsp